Catal Lett (2012) 142:566–572
DOI 10.1007/s10562-012-0802-8

Ultrahigh Active Pd Nanocatalyst Supported on Core-Sheath Conducting Polymer/Metal Oxide Composite Nanorods

Xiaofeng Lu · Yanpeng Xue · Guangdi Nie · Ce Wang

Received: 2 January 2012 / Accepted: 7 March 2012 / Published online: 29 March 2012

Abstract A facile and aqueous-phase method based on the electron transfer reduction process for fabricating core-sheath structured polyaniline (PANI)/SnO_2 composite nanorods supported Pd nanocatalyst has been demonstrated. The Pd nanoparticles synthesized by this strategy have a small size of smaller than 3.0 nm. The well dispersed Pd nanoparticles with small sizes supported on core-sheath PANI/SnO_2 composite nanorods exhibited an ultrahigh catalytic activity during the catalytic reduction of *p*-nitrophenol into *p*-aminophenol by $NaBH_4$ in aqueous solution. The kinetic apparent rate constant (k_{app}) reach to be about 26.9×10^{-3} s^{-1}. It is believed that this method could be extended to cover many kinds of other functional composite nanomaterials where the active component is expected to bring in new features and applications.

Keywords Electron transfer reduction · Polyaniline · Tin oxide · Palladium · Catalysis

1 Introduction

Noble metal nanoparticles with controllable sizes and shapes have attracted growing attention for their unique physical and chemical properties and potential applications in catalysis, sensors, information storage, surface enhanced Raman scattering, biomedicine, and so on [1–11]. Especially, metal nanoparticles become more and more important in catalytic applications because of their large surface area and super-high activity. However, the metal nanoparticles with small size are easily aggregated for the high surface energy, reducing their catalytic activity. To overcome this problem, metal nanoparticles are often immobilized onto some less expensive solid supports, such as metal oxides, carbon and polymers, etc. [12–20]. Moreover, the deposition of metal nanoparticles on metal oxide supports often exhibit enhanced catalytic activity and selectivity because of the synergistic effect between them [21–23]. Early reports on the fabrication of metal nanoparticles onto metal oxide support mainly involved the calcination of metal precursors on the surface or inside metal oxide nanostructures at a high temperature [24–26]. However, the metal nanoparticles produced by this method are often poorly dispersed on the support. Therefore, it is still a challenge to develop a facile method to fabricate composite nanostructures consisting highly dispersed metal nanoparticles onto the metal oxide matrix.

Among various metal/metal oxide composite nanostructures, supported Pd nanocatalysts have been found to play an important role for a number of reactions, including hydrogenation reaction, the carbon–carbon cross-coupling reaction, the oxidation of primary alcohols, the direct generation of H_2O_2 from H_2 and O_2, and so on [27–30]. Recently, Lee et al. [31] reported the preparation of Pd/SnO_2 composite nanorods by using $NaBH_4$ as reducing agent via a solution process, but the size of the Pd nanoparticles is large, limited their applications in the catalysis. Here, we report a simple and water-phase route for the synthesis of a polyaniline (PANI)/SnO_2/Pd tri-component hybrid nanorod consisting of sub-3 nm Pd nanocrystals supported on core-sheath PANI/SnO_2 nanorods with a out-diameter of about 100–150 nm through an electron transfer reduction process. It is well known that the oxidation

X. Lu (✉) · Y. Xue · G. Nie · C. Wang (✉)
Alan G. MacDiarmid Institute, College of Chemistry, Jilin University, Changchun 130012, China
e-mail: xflu@jlu.edu.cn

C. Wang
e-mail: cwang@jlu.edu.cn

potential of PANI is much higher than that of the palladium ions, so PANI/Pd composites could be simply synthesized by directly mixing the PANI and palladium ions via a redox reaction [32, 33]. However, the size of Pd nanoparticles supported on PANI matrix is too large via such a direct redox reduction method because the growth is fast. To prevent the Pd nanocrystals grow too fast, we have synthesized a core-sheath PANI/SnO_2 composite nanorods firstly. Then they were mixed with Na_2PdCl_2 to generate small Pd nanocrystals supported on the core-sheath PANI/SnO_2 composite nanorods by an electron transfer reduction process. Using this approach, we were able to synthesize PANI/SnO_2/Pd composite nanorods with good dispersion of Pd nanocrystals in high yields. This procedure is simple and mass-produced, because it does not require high temperature calcination or other reducing agents. It was found that the as-prepared PANI/SnO_2/Pd composite nanorods exhibit an ultrahigh activity as catalysts for the reduction of *p*-nitrophenol by sodium borohydride ($NaBH_4$) at ambient conditions.

2 Experimental

2.1 Chemicals

Aniline monomer was distilled under reduced pressure before use. All the other chemicals were of analytical grade and used as received without further purification.

2.2 Synthesis of PANI Nanorods

The preparation of PANI nanorods was according to previous report [34]. In a typical procedure, an aqueous solution of 0.3 mL aniline monomer in 10 mL of 1.0 M HCl and another aqueous solution of 0.18 g ammonium peroxydisulfate in 10 mL of 1.0 M HCl were prepared and mixed rapidly. After shaking for about 30 s, the mixture was left for 2 h. The obtained green precipitate was centrifuged and washed with deionized water and ethanol for several times. At last, it was dried in vacuum at 40 °C for one night.

2.3 Preparation of Core-Sheath PANI/SnO_2 Composite Nanorods

The core-sheath PANI/SnO_2 composite nanorods were prepared by the hydrolysis of $SnCl_2$ on the surface of PANI nanorods. Typically, 30 mg of PANI nanorods were dispersed in 18 mL of water containing 0.15 mL HCl at room temperature. Then 0.66 g of $SnCl_2{\cdot}2H_2O$ and 0.3 g urea were added into the above solution. The mixture was continually stirred at 60 °C for 6 h. The obtained jade-green product was centrifuged and washed with water and ethanol for several times, then the product was dried at 40 °C under vacuum for one night.

2.4 Preparation of PANI/SnO_2/Pd Composite Nanorods

The PANI/SnO_2/Pd composite nanorods were prepared by the reduction of $NaPdCl_4$ via an electron transfer process. Briefly, 5 mg of the as-prepared core-sheath PANI/SnO_2 composite nanorods were dispersed into 10 mL of water. After that, 1 mL aqueous solution containing 5 mg $NaPdCl_4$ was added into the above reactive medium. The reaction was going on for about 5 h. The product was centrifuged and then washed with water and ethanol for several times. At last, the product was dried at 40 °C under vacuum for one night.

2.5 Reduction of *p*-Nitrophenol Catalyzed by PANI/SnO_2/Pd Composite Nanorods

Typically, the aqueous solution of *p*-nitrophenol (1.7 mL, 2.0×10^{-4} M) and $NaBH_4$ (1.0 mL, 1.5×10^{-2} M) were added together into a quartz cuvette. Then, 0.3 mL of an aqueous solution containing PANI/SnO_2/Pd composite nanorods (0.224 mg/mL) was injected into the cuvette to start the reaction. The intensity of the absorption peak at 400 nm in ultraviolet–visible (UV–Vis) spectroscopy was used to monitor the process of the conversion of *p*-nitrophenol to *p*-aminophenol.

2.6 Characterization

Transmission electron microscopy (TEM) experiments were performed on JEM-1200 EX (JEOL) electron microscopes with an acceleration voltage of 100 kV. High-resolution TEM (HRTEM) imaging and energy-dispersive X-ray (EDX) analysis were performed on a FEI Tecnai G2 F20 high-resolution transmission electron microscope operating at 200 kV. Fourier transform infrared (FTIR) spectra of KBr powder-pressed pellets were recorded on a BRUKER VECTOR 22 Spectrometer. UV–Vis spectra were recorded on a Shimadzu UV-2501 PC spectrometer. Analysis of the X-ray photoelectron spectra (XPS) was performed on an ESCLAB MKII using Al as the exciting source. The weight percent of Pd in the nanocomposites was determined by inductively coupled plasma (ICP) atomic emission spectrometric analysis (POEMS, TJA).

3 Results and Discussion

In this study, PANI nanorods were synthesized by a rapid mixing method through the oxidation polymerization between aniline monomer and the oxidant ammonium

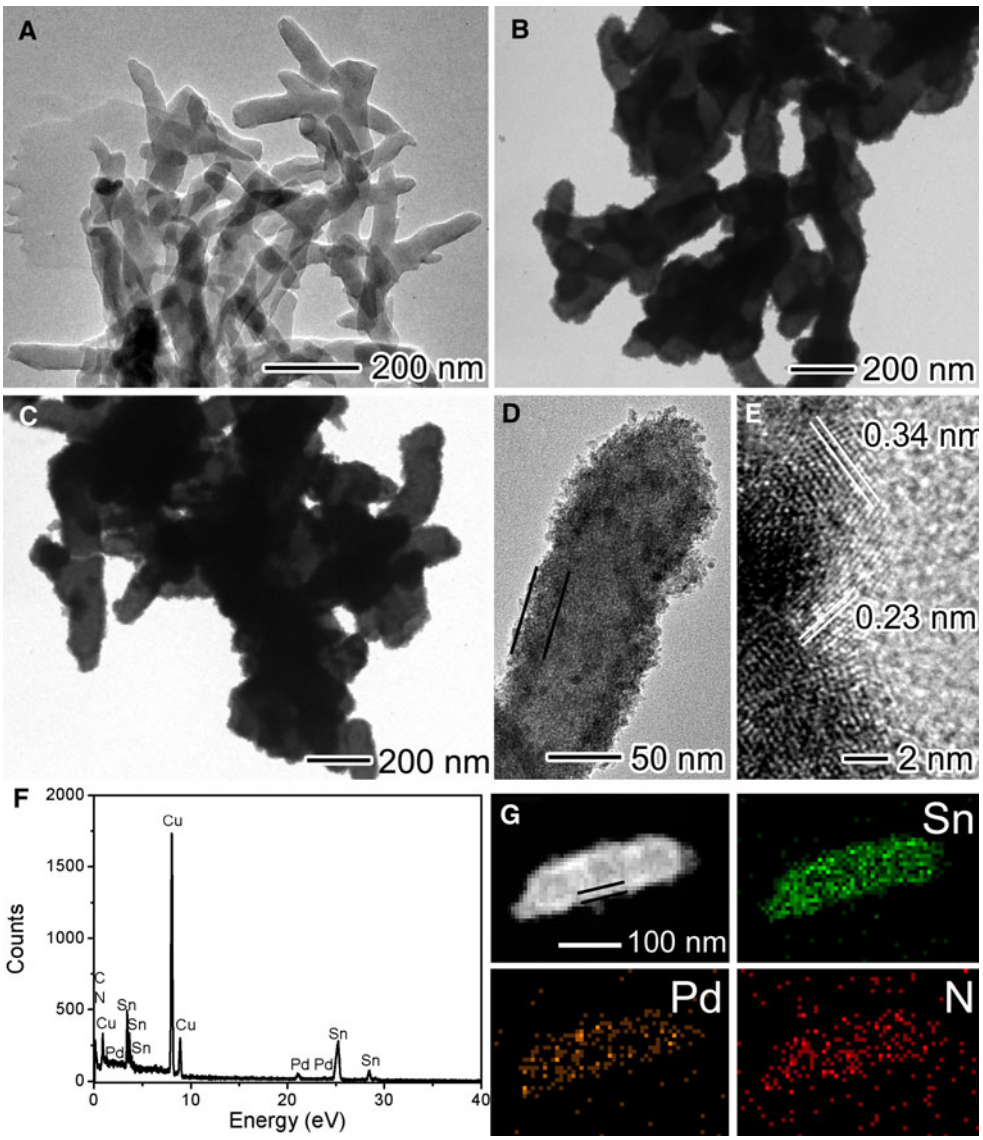

Fig. 1 **A** TEM image of PANI nanorods synthesized via a rapid mixing polymerization method. **B** TEM image of PANI/SnO_2 composite nanorods obtained by the hydrolysis of $SnCl_2$. **C** TEM image of PANI/SnO_2/Pd composite nanorods obtained by electron transfer reducing Na_2PdCl_4 with PANI nanorods in a aqueous solution. **D**, **E** HRTEM images of PANI/SnO_2/Pd composite nanorods. **F** EDX analysis of PANI/SnO_2/Pd composite nanorods. **G** EDX mapping images of PANI/SnO_2/Pd composite nanorods

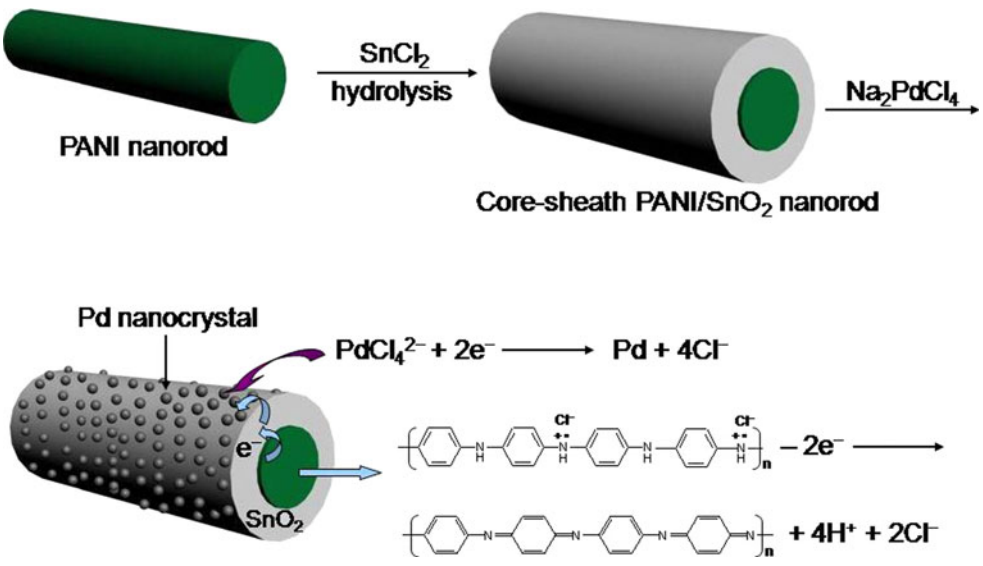

Fig. 2 Schematic illustration of the fabrication of PANI/SnO_2/Pd composite nanorods via an electron transfer reducing process

peroxide, as reported previously [34]. Figure 1A shows a TEM image of as-prepared PANI nanorods. It was found that they were uniform with a diameter about 50 nm and a length of several hundred nanometers. After coating with SnO_2, the PANI nanorods are homogeneously encapsulated by a SnO_2 layer with the thickness of about 20–30 nm. The formation of SnO_2 layer on the surface of PANI nanorods could be attributed to the hydrolysis of $SnCl_2$ to form SnO_2 nanocrystals and spontaneously formed on the surface of PANI nanorods. From Fig. 1B, it was found that the SnO_2 layer on the surface of PANI nanorods was compact and form a core-sheath structure. These core-sheath PANI/SnO_2 composite nanorods were then used as supports for the preparation of PANI/SnO_2/Pd composite nanostructures. Pd nanocrystals were directly grown on the surface of PANI/SnO_2 nanorods upon the reduction of $PdCl_4^{2-}$ by the electrons generated from PANI in an aqueous solution. Figure 1C shows a typical image of the PANI/SnO_2/Pd composite nanorods, revealing that the morphology of the product does not change after the formation of Pd nanocrystals on their surface, and there are not isolated Pd nanocrystals in the product. To further prove the formation of the PANI/SnO_2/Pd composite nanorods, HRTEM images were shown in Fig. 1D and E, which clearly exhibits the formation of most of Pd nanocrystals with sizes of 1–3 nm on the surface of core-sheath PANI/SnO_2 composite nanorods. The lattice spacing of 0.34 and 0.23 nm corresponds to those {110} facets of SnO_2 and {111} facets of Pd, respectively. From HRTEM image, it was also found the formation of the metal–metal oxide interface because no large capping agents formed on the surface of Pd nanocrystals by using our method. The strong metal–metal oxide interaction would increase the activation energy for some catalytic reactions [35]. The overall weight percentage of Pd in the PANI/SnO_2/Pd composite nanorods was 7.9 %, which was determined by ICP atomic spectrum measurements. As shown in Fig. 1F, the energy-dispersive X-ray spectroscopy (EDS) also confirms that the element of Pd, Sn, C, N exists in the PANI/SnO_2/Pd composite nanorods, and no other obvious element is observed except Cu. The signal of Cu in the EDS spectrum originates from the carbon-coated copper grid. All results demonstrate the feasibility of our approach for the preparation of PANI/SnO_2/Pd composite nanorods.

The mechanism of the formation of Pd nanocrystals on the surface of core-sheath PANI/SnO_2 composite nanorods could be explained in two ways. The first explanation is that $PdCl_4^{2-}$ will diffuse into the interface between SnO_2 layer and PANI matrix where it could be reduced by PANI nanorods to form Pd nanocrystals. In this case, Pd nanoparticles would be formed homogeneously at the interface between SnO_2 layer and PANI nanorods or inside PANI nanorods, and not formed on the outside of the surface of

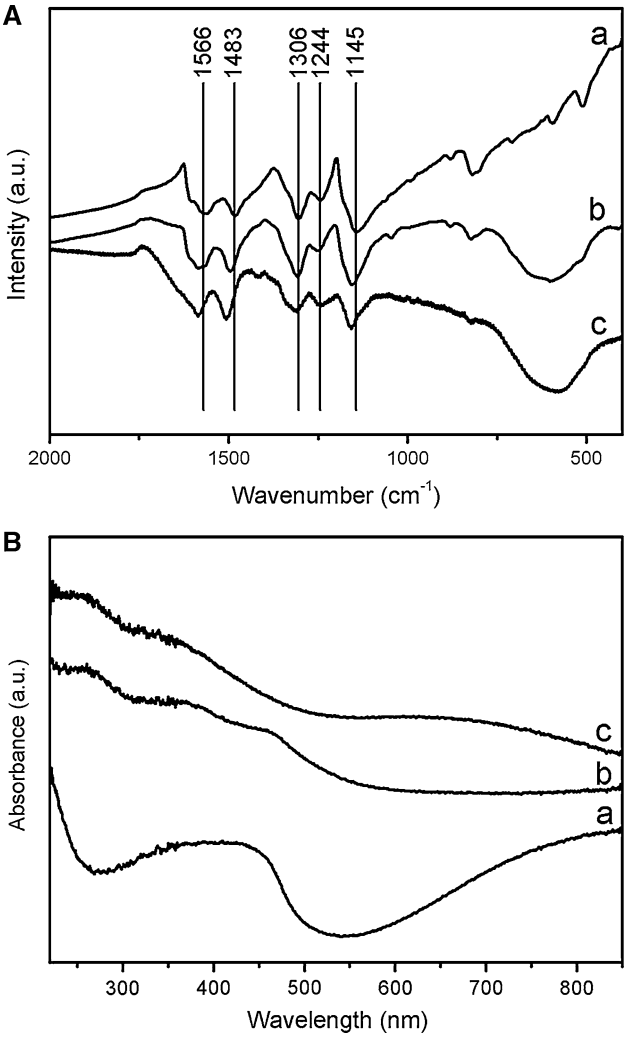

Fig. 3 **A** FTIR spectra of (*a*) PANI nanorods, (*b*) core-sheath PANI/SnO_2 composite nanorods and (*c*) PANI/SnO_2/Pd composite nanorods; **B** UV–Vis absorption spectra (*a*) PANI nanorods, (*b*) the as-prepared core-sheath PANI/SnO_2 composite nanorods and (*c*) PANI/SnO_2/Pd composite nanorods

SnO_2 layers. However, Fig. 1G strongly contradicts this hypothesis, which the EDX elemental-mapping analysis revealed that Pd atoms were homogeneously distributed throughout the surface of core-sheath PANI/SnO_2 composite nanorods. Therefore, we think that Pd nanocrystals should be in situ reduced on the surface of PANI/SnO_2 composite nanorods by an electron transfer reduction process, which is similar with the previous report [36]. When $PdCl_4^{2-}$ was mixed with PANI/SnO_2 composite nanorods, PANI will be oxidized to generate electrons, which will be transferred through the semiconductor SnO_2 layer to its surface, where the $PdCl_4^{2-}$ are reduced by the released electrons to form Pd nanocrystals (Fig. 2). Compared to the method by the directly mixing PANI nanorods and $NaPdCl_4^{2-}$, this process provides the preparation of Pd nanoparticles with a small size [32, 33].

The chemical composition of the as-prepared PANI/SnO_2/Pd composite nanorods was supported by the FTIR and UV–Vis absorption spectroscopies. Figure 3A shows typical FTIR spectra of PANI nanorods, the as-synthesized PANI/SnO_2 and PANI/SnO_2/Pd composite nanorods, respectively. For PANI nanorods, the peaks at 1,566 and 1,483 cm^{-1} are ascribed to the characteristic C=C stretching of the quinonoid and benzenoid rings, respectively. The peaks at 1,306 and 1,244 cm^{-1} are corresponding to C–N and C=N stretching vibrations. The peak at 1,145 cm^{-1} is related to the in-plane bending of C–H. Compared to PANI nanorods, a new broad peak at about 600 cm^{-1} has appeared in PANI/SnO_2 and PANI/SnO_2/Pd composite nanorods, which are assigned to the Sn–O–Sn vibration, indicating the formation of SnO_2 layer [37]. In addition, the ratio of the relative intensity of the peaks corresponding to C=N and C–N stretching vibrations increases significantly after the formation of Pd nanocrystals, showing that PANI was partially oxidized via an electron transfer process. The oxidation state of PANI after the electron transfer reduction process was also proved by the UV–Vis spectra. For PANI nanorods, the absorption peaks at 320–360 nm could be attributed to the π–π^* electron transition, and the absorption bands at 400–420 and $\sim$800 nm could be ascribed to doping level and formation of polaron, respectively [38]. After coating with SnO_2 and Pd nanocrystals, a new broad peak at 570–670 nm appeared, indicating the formation of emeraldine and pernigraniline base of PANI, which also proved the oxidation of PANI [39].

The oxidation state of Pd nanocrystals in the PANI/SnO_2/Pd composite nanorods is determined by XPS as shown in Fig. 4. The XPS spectrum of the as-synthesized PANI/SnO_2/Pd composite nanorods exhibits characteristic signals for $Pd3d_{5/2}$ and $Pd3d_{3/2}$ and the elements of Sn, O, C, N were also observed, which is consistent with the EDX analysis. The Pd3d peaks could be deconvoluted into two components, which are corresponding to the two oxidation states of Pd in the PANI/SnO_2/Pd composite nanorods. The peaks at 335.6 eV ($Pd3d_{5/2}$) and 341.0 eV ($Pd3d_{3/2}$) are assigned to Pd(0), and the other peaks at 338.2 eV ($Pd3d_{5/2}$) and 343.5 eV ($Pd3d_{3/2}$) are related to the oxidized palladium(II) centers [40]. Previous studied also showed that oxidized palladium were consistent with Pd nanocrystals when the size of Pd nanocrystals are small (2.5 nm or less) [41]. As shown in Fig. 4B, $Sn3d_{5/2}$ and $Sn3d_{3/2}$ doublet with the binding energies of 495.6 and 487.2 eV are observed, respectively, indicating that SnO_2 is coated on the surface of PANI nanorods. The N1s spectrum could be deconvoluted into two components, with binding energy at 400.3 and 399 eV. The former peak is attributed to neutral nitrogen moieties in PANI [42]. The signal of 399 eV is usually ascribed to uncharged deprotonated imine (=N–) atoms [42], which is also consistent with the process of the oxidation of PANI by $PdCl_4^{2-}$.

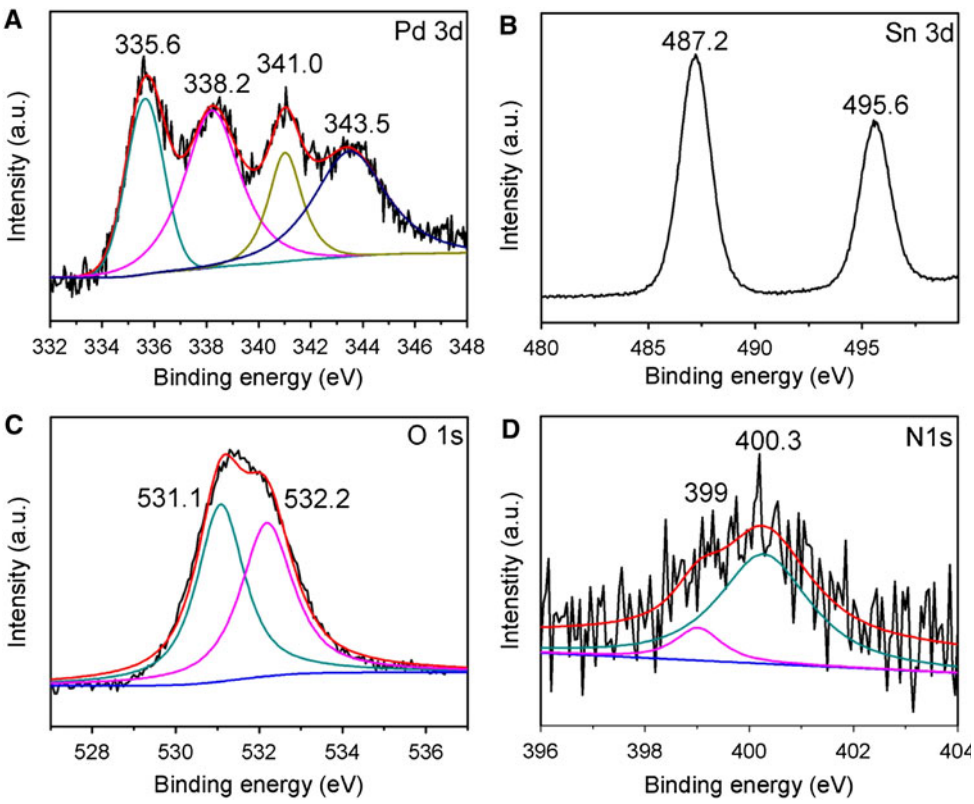

Fig. 4 XPS spectra of the as-synthesized PANI/SnO_2/Pd composite nanorods, **A** Pd3d, **B** Sn3d, **C** O1s, **D** N1s

It is well known that Pd is an excellent catalyst for hydrogenation reactions. In this study, we evaluated the catalytic activity of the PANI/SnO_2/Pd composite nanorods by using a well-known catalytic reaction involving the reduction of *p*-nitrophenol into *p*-aminophenol with an excess amount of $NaBH_4$ in aqueous solution as a model system. The *p*-nitrophenol solution exhibited an absorption peak at $\lambda_{max} = 400$ nm in the presence of $NaBH_4$, corresponding to its ions in alkaline conditions. The intensity of this peak as a function of time could be used to monitoring the kinetic process of the reduction process. After the PANI/SnO_2/Pd composite nanorods was added into the reaction system, the characteristic absorption peak of *p*-nitrophenolate ion at 400 nm decreased gradually and disappeared within 100 s, while a new peak at 298 nm which ascribed to the *p*-aminophenol emerged. Correspondingly, the yellow color of the *p*-nitrophenolate ions diminished after 100 s, indicating that *p*-nitrophenol had been completely converted to *p*-aminophenol. In this experiment, $NaBH_4$ was in excess in the reaction system, so the reduction process could be regarded as pseudo-first-order with respect to the concentration of *p*-nitrophenolate. Since the absorbance of *p*-nitrophenolate is proportional to its concentration in the system, the ratios of *p*-nitrophenolate concentrations at time t (C_t) to its initial value at time 0 (C_0) can be stranded for the relative intensity of the respective absorbance A_t/A_0. As shown in Fig. 5, a linear relationship between $\ln(C_t/C_0)$ and reaction time for the reduction of *p*-nitrophenol catalyzed by PANI/SnO_2/Pd composite nanorods was obtained. It was observed that the reaction could be complete within 100 s in the presence of excess $NaBH_4$. However, the reaction would be complete in 300 s for the reduction of *p*-nitrophenol by using SnO_2/Pd nanocatalyst, indicating the catalytic activity of PANI/SnO_2/Pd nanocatalyst was much better. The SnO_2/Pd nanocatalyst was prepared by reducing Pd nanoparticles on the surface of electrospun SnO_2 nanofibers by $NaBH_4$. The kinetic apparent rate constant (k_{app}) for the reduction of *p*-nitrophenol by using the PANI/SnO_2/Pd nanocatalyst was calculated to be about 26.9×10^{-3} s^{-1}, which was also much higher than most of the other substrate supported noble metal nanocatalysts [15, 43–47]. The Pd nanocrystals with small sizes were well dispersed on the surface of core-sheath PANI/SnO_2 composite nanorods, affording effective contact between the catalysts and the reactants in the reaction. Therefore, the PANI/SnO_2/Pd composite nanorods exhibited an ultrahigh catalytic efficiency towards the reduction of *p*-nitrophenol.

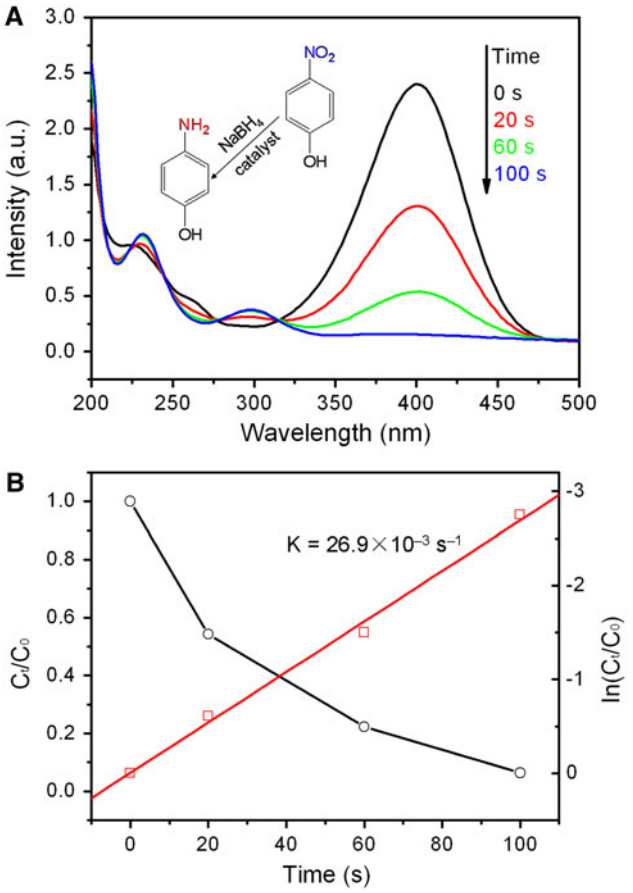

Fig. 5 **A** UV-Vis absorption spectra for the catalytic reduction of *p*-nitrophenol by $NaBH_4$ over PANI/SnO_2/Pd composite nanorods. **B** The circles and squares stand for the C_t/C_0 and $\ln(C_t/C_0)$ versus reaction time for the reduction of *p*-nitrophenol by $NaBH_4$ over PANI/SnO_2/Pd composite nanorods, respectively. C_0 stands for the intensity of the absorption at 400 nm initially and C_t was the absorption peak at time t

4 Conclusions

In conclusion, for the first time, core-sheath structured PANI/SnO_2 composite nanorods were used to stabilize Pd nanocatalysts by a facile, aqueous-phase in situ electron transfer reduction method. The well dispersed Pd nanocrystals with small sizes supported on core-sheath PANI/SnO_2 composite nanorods exhibited an ultrahigh catalytic activity during the catalytic reduction of *p*-nitrophenol into *p*-aminophenol by $NaBH_4$ in aqueous solution. The obtained PANI/SnO_2/Pd composite nanorods in this work may be found use in many other applications such as electrocatalysis, sensors, energy conversion, and so on. In addition, this approach is expected to be extendible to prepare other kinds of composite systems.

Acknowledgments This work was supported by the research grants from the National 973 Project (S2009061009), the National Natural Science Foundation of China (20904015, 50973038), Jilin Science and Technology Department project (20100101, 201115014) and State Key Laboratory for Modification of Chemical Fibers and Polymer Materials, Dong Hua University.

References

1. Xia YN, Xiong YJ, Lim B, Skrabalak SE (2009) Angew Chem Int Ed 48:60
2. Lewis LN (1993) Chem Rev 93:2693
3. Somorjai GA (1996) Chem Rev 96:1223
4. Taton TA, Mirkin CA, Letsinger RL (2000) Science 289:1757
5. Tkachenko AG, Xie H, Coleman D, Glomm W, Ryan J, Anderson MF, Franzen S, Feldheim DL (2003) J Am Chem Soc 125:4700
6. Wang H, Brandl DW, Nordlander P, Halas NJ (2007) Acc Chem Res 40:53
7. Murray CB, Sun S, Doyle H, Betley T (2001) MRS Bull 26:985
8. Nie S, Emory SR (1997) Science 275:1102
9. West JL, Halas NJ (2003) Annu Rev Biomed Eng 5:285
10. Skrabalak SE, Chen J, Au L, Lu X, Li X, Xia Y (2007) Adv Mater 19:3177
11. Jain PK, El-Sayed IH, El-Sayed MA (2007) Nano Today 2:18
12. Chen MS, Goodman DW (2004) Science 306:252
13. Xu C, Xie J, Ho D, Wang C, Kohler N, Walsh EG, Morgan JR, Chin YE, Sun S (2008) Angew Chem Int Ed 47:173
14. Yu T, Zeng J, Lim B, Xia YN (2010) Adv Mater 22:5188
15. Zhang ZY, Shao CL, Zou P, Zhang P, Zhang MY, Mu JB, Guo ZC, Li XH, Wang CH, Liu YC (2011) Chem Commun 47:3906
16. Zhang P, Shao CL, Zhang ZY, Zhang MY, Mu JB, Guo ZC, Liu YC (2011) Nanoscale 3:3357
17. Hu XG, Wang T, Qu XH, Dong SJ (2006) J Phys Chem B 110:853
18. Wunder S, Polzer F, Lu Y, Mei Y, Ballauff M (2010) J Phys Chem C 114:8814
19. Tamai T, Watanabe M, Teramura T, Nishioka N, Matsukawa K (2010) Macromol Symp 288:104
20. Zinovyeva VA, Vorotyntsev MA, Bezverkhyy I, Chaumont D, Hierso JC (2011) Adv Funct Mater 21:1064
21. Huang PX, Wu F, Zhu BL, Gao XP, Zhu HY, Yan TY, Huang WP, Wu SH, Song DY (2005) J Phys Chem B 109:19169
22. Formo E, Peng Z, Lee E, Lu X, Yang H, Xia Y (2008) J Phys Chem C 112:9970
23. Lee YM, Garcia MA, Huls NAF, Sun SH (2010) Angew Chem Int Ed 49:1271
24. Brogan MS, Dines TJ (1994) J Chem Soc Faraday Trans 90:1461
25. Abid M, Ehret G, Touroude R (2001) Appl Catal A 217:219
26. Takahashi M, Mori T, Ye F, Vinu A (2007) J Am Ceram Soc 90:1291
27. Kang JH, Shin EW, Kim WJ, Park JD, Moon SH (2002) J Catal 208:310
28. Cwik A, Hell Z, Figueras F (2005) Org Biomol Chem 3:4307
29. Ebitani K, Fujie Y, Kaneda K (1999) Langmuir 15:3557
30. Park S, Seo JG, Jung JC, Baeck SH, Kim TJ, Chung YM, Oh SH, Song IK (2009) Catal Commun 10:1762
31. Lee JM, Park J, Kim S, Kim S, Lee E, Kim SJ, Lee W (2010) Int J Hydrog Energy 35:12568
32. Gallon BJ, Kojima RW, Kaner RB, Diaconescu PL (2007) Angew Chem Int Ed 46:7251
33. Gao Y, Chen CA, Gau HM, Bailey JA, Akhadov E, Williams D, Wang HL (2008) Chem Mater 20:2839
34. Huang JX, Kaner RB (2004) Angew Chem Int Ed 43:5817
35. Contreras AM, Yan X-M, Kwon S, Bokor J, Somorjai GA (2006) Catal Lett 111:5
36. Song W, Han XX, Chen L, Yang YM, Tang B, Ji W, Ruan WD, Xu WQ, Zhao B, Ozaki Y (2010) J Raman Spectrosc 41:907
37. Monredon S, Cellot A, Ribot F, Sanchez C, Armelao L, Gueneau L, Delattre L (2002) J Mater Chem 12:2396
38. Stejskal J, Kratochvil P, Radhakrishnan N (1993) Synth Met 61:225
39. Kang ET, Neoh KG, Tan KK (1998) Prog Polym Sci 23:277
40. Hierso J–C, Satto C, Feurer R, Kalck P (1996) Chem Mater 8:2481
41. Frenkel AI, Hills CW, Nuzzo RG (2001) J Phys Chem B 105:12689
42. Atanasoska L, Naoi K, Smyrl WH (1992) Chem Mater 4:988
43. Han J, Li LY, Guo R (2010) Macromolecules 43:10636
44. Jiang HL, Akita T, Ishida T, Haruta M, Xu Q (2011) J Am Chem Soc 133:1304
45. Koga H, Tokunaga E, Hidaka M, Umemura Y, Saito T, Isogai A, Kitaoka T (2010) Chem Commun 46:8567
46. Tang S, Vongehr S, Meng X (2010) J Mater Chem 20:5436
47. Esumi K, Isono R, Yoshimura T (2004) Langmuir 20:237